Preparation and Characterization of Porous Poly(vinylidene fluoride) Membranes for Dehumidification with Poly(ethylene glycol) as an Additive

Lixia Pei, Weijie Zhao, Lizhi Zhang

Key Laboratory of Enhanced Heat Transfer and Energy Conservation of Education Ministry, School of Chemistry and Chemical Engineering, South China University of Technology, Guangzhou, China 510640

Received 22 January 2010; accepted 12 April 2010
DOI 10.1002/app.32628
Published online 29 June 2010 in Wiley InterScience (www.interscience.wiley.com).

ABSTRACT: Porous poly(vinylidene fluoride) (PVDF) membranes for dehumidification were prepared from a PVDF/dimethylformamide/water system by phase inversion with poly(ethylene glycol) (PEG) as an additive at various concentrations (1.2, 1.8, and 2.4%) and with various molecular weights (1000, 2000, and 6000). The surface morphologies of the resultant membranes were characterized with scanning electron microscopy and atomic force microscopy, and the pore diameter, porosity, and pore size distribution of the membranes were also determined by a gas-sorption method. The influence of the concentration and molecular weight of PEG on water-vapor transport through the membranes was evaluated. The moisture-transport property of the membranes was improved significantly with increases in the concentration and molecular weight of PEG, and a membrane with good moisture permeability was obtained with 2.4% PEG-6000 as an additive. © 2010 Wiley Periodicals, Inc. J Appl Polym Sci 118: 2696–2703, 2010

Key words: additives; fluoropolymers; membranes; polymer blends

INTRODUCTION

Membrane-based dehumidification is widely applied in the drying of natural gas and organic vapors and in humidity control in closed spaces because of its low cost and low energy consumption.[1] Diverse membranes have been successfully developed for dehumidification. For instance, supported liquid membranes have been applied to remove moisture from air or gases because of its good selectivity for water vapor with respect to air. Several types of supported liquid membranes were reported by Ito and coworkers,[2–4] and composite supported liquid membranes have also been used to improve membrane stability.[5] Moreover, composite membranes, comprising a dense active layer and a porous substrate, are widely recommended for obtaining high permeability and selectivity. The thin active layer provides permselectivity to the membranes, whereas the porous substrate acts as mechanical support. Various hydrophilic membranes have been investigated as active layers for composite membranes for dehumidification.[6–8] Apart from the active layer, the microstructure of the substrate also plays an important role in the permeation performance of composite membranes.[9–11]

Typically, the substrate of composite membranes for dehumidification needs low resistance as well as good strength, so porous membranes are extensively used as substrates. Porous membranes are generally prepared by phase inversion. In this process, the microstructure and properties of the membranes are dependent on many factors, including the additives, polymer concentration, solvent, and coagulation bath. The addition of additives to a casting solution is a convenient and efficient method of obtaining membranes with desirable pore structures and high permeation properties.

In general, these additives mainly include water-soluble inorganic salts such as LiCl/$ZnCl_2$, organic small molecules, and polymers such as glycerol, polyvinylpyrrolidone (PVP), and poly(ethylene glycol) (PEG). In comparison, polymer additives are widely used for the fabrication of porous membranes.

Correspondence to: L. Zhang (lzzhang@scut.edu.cn).
Contract grant sponsor: National Natural Science Foundation of China; contract grant number: 50676034.
Contract grant sponsor: Fundamental Research Funds for the Central Universities; contract grant number: 2009ZZ0060.
Contract grant sponsor: National Key Project of Scientific and Technical Supporting Programs; contract grant number: 2006BAA04B02.

Membranes with desirable microstructures have been prepared by the variation of the amount or molecular weight of PEG or PVP.[12–20] For instance, Idris et al.[18] found that the addition of high-molecular-weight PEG enlarged the pore size and enhanced the pure water permeation of poly(ether sulfone) ultrafiltration membranes. Chakrabarty et al.[19,20] observed an increasing tendency for pure water flux in polysulfone (PSf) ultrafiltration membranes with the PEG molecular weight increasing from 400 to 20,000.

Although many reports on the fabrication of porous membranes with PEG or PVP as an additive have appeared, porous membranes have been applied mainly in the field of microfiltration/ultrafiltration. For the support layer of composite membranes for dehumidification, high moisture permeability and good strength are the number one issues. However, there are relatively few concerns about the preparation of porous membranes as substrates for composite membranes for dehumidification. The effect of additives on the transport of water vapor through porous membranes has not been discussed and studied.

Poly(vinylidene fluoride) (PVDF) is widely used to prepare porous membranes for the substrates of composite membranes because of its excellent mechanical properties, good thermal and chemical stability, and cheapness. In this study, to obtain an excellent substrate for composite membranes for dehumidification, porous PVDF membranes with various morphologies were prepared by phase inversion with PEGs of different molecular weights. Moreover, the effects of the PEG additives on the morphology and water-vapor transport of the porous PVDF membranes were investigated in detail.

EXPERIMENTAL

Materials

PVDF (weight-average molecular weight = 300,000) was supplied by Xilai Fine Chemical Co., Ltd. (Tianjin, China). PEG (weight-average molecular weight = 1000, 2000, or 6000) was purchased from Guanghua Chemical Co., Ltd. (Shantou, China). *N,N*-Dimethylformamide (DMF) was used without further purification. Tap water was used as the nonsolvent in the coagulation bath.

Membrane preparation

Flat-sheet, porous PVDF membranes were prepared by phase inversion. The required amount of PVDF was dissolved in DMF along with an appropriate amount of PEG at 50°C to form a casting solution (PEGs of various molecular weights were used for the different membranes); then, the solution was kept at room temperature for 24 h. The compositions of the casting solutions for the different membranes are shown in Table I. After debubbling, the solutions were coated uniformly onto clean glass plates, and the thickness of the membranes was controlled by the gap between the casting knife and glass plate. Then, the solution films were immersed immediately in a coagulation bath of tap water at room temperature. The formed membranes were peeled off and were washed thoroughly with water subsequently to remove the residual solvent. The desired membranes were produced with 24 h of drying at room temperature.

TABLE I
Compositions of the Casting Solutions for the Preparation of Different Membranes

	PEG (wt %)			PVDF	DMF
Membrane	PEG-1000	PEG-2000	PEG-6000	(wt %)	(wt %)
M1	—	1.2	—	9	89.8
M2	—	1.8	—	9	89.2
M3	—	2.4	—	9	88.6
M4	2.4	—	—	9	88.6
M5	—	—	2.4	9	88.6

Characterization of the membranes

Membrane morphology

The surface morphology of the prepared porous membranes was observed with scanning electron microscopy (SEM; 1530 VP, Leo, Oberkochen, Germany) after they were coated with gold. The surface topography of the porous membranes was observed with atomic force microscopy (AFM; CSPM-2003, Benyuan Ltd, Beijing, China). The AFM images were obtained in a contact mode in the scan area of 5 μm × 5 μm under ambient conditions.

Gas (N_2) sorption test

The average pore size, porosity, and pore size distribution of the membranes were quantitatively determined by a gas (N_2) sorption method with accelerated surface area and pore (ASAP) analysis (ASAP 2010, Micromeritics Instrument corporation, Norcross, GA). The cumulative volume and cumulative surface area of the pores were measured by ASAP analysis. With the Barrett–Joyner–Halendar model (based on the Kelvin equation describing the capillary condensation phenomenon in a cylindrical pore),[21] the pore size distribution was estimated from the desorption branch of the isotherm with the following equations.

The pore size distribution [$f(\lambda)$] was defined as the fraction of pores with diameter λ_I:

$$f(\lambda) = \frac{N_I}{\sum_{I=1}^{I=J} N_I} \quad (1)$$

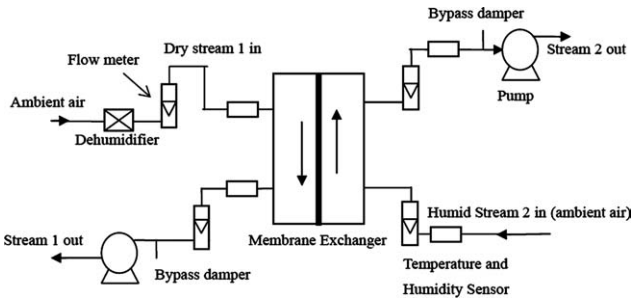

Figure 1 Experimental setup.

where N_I is the number of pores of diameter λ_I. The cumulative volume of pores of diameter λ_I (VP_I) was calculated as follows:

$$VP_I = \pi(Lp_I)\left[\frac{\lambda_I}{2}\right]^2 N_I \tag{2}$$

where Lp_I is the pore length (approximately equivalent to the thickness of the measured membrane).

The cumulative surface area of pores of diameter λ_I (SA_I) was calculated as follows:

$$SA_I = \pi Lp_I \lambda_I N_I \tag{3}$$

Rearrangement of eqs. (2) and (3) and substitution into eq. (1) provided the following:

$$f(\lambda) = \frac{{SA_I}^2/VP_I}{\sum_{I=1}^{I=J} {SA_I}^2/VP_I} \tag{4}$$

The average pore diameter (λ_m) was calculated as follows:

$$\lambda_m = \sqrt{\frac{4A_{\text{pore}}}{\pi N_t}} \tag{5}$$

where A_{pore} is the total pore area and N_t is the total number of pores.

The surface porosity (ε) was calculated as the summation of A_{pore} divided by the area of the measured membrane (A_t) as follows:[20]

$$\varepsilon = \frac{A_{\text{pore}}}{A_t} \tag{6}$$

Water-vapor-transport performance measurement

In a way similar to a previously described method,[8] the water-vapor-transport performance was measured in a test rig (Fig. 1) in terms of the total mass transport coefficient (K) and moisture permeation rate (Pe).

In the test rig, two streams, one dry and one humid, flowed through a membrane exchanger to exchange moisture. In this work, for the dry stream, ambient air was dehumidified and then was drawn to the exchanger. For the humid stream, it was driven directly from the ambient atmosphere to the exchanger. According to the measured inlet and outlet humidity in different flows, K and Pe were obtained with the following equations.

K (m/s) was calculated as follows:

$$K = \frac{\Delta W}{\rho_a A \Delta\omega_m} \tag{7}$$

where A is the transport area of the membrane in the cell (m^2), ρ_a is the air density (kg/m^3), ΔW is the mass of vapor transported through the membrane (kg/s), and $\Delta\omega_m$ is the logarithmic mean humidity difference. ΔW and $\Delta\omega_m$ were calculated separately with eqs. (8) and (9):

$$\Delta W = \frac{V\rho_a}{3600}\left[\frac{(\omega_{1o} - \omega_{1i}) + (\omega_{2i} - \omega_{2o})}{2}\right] \tag{8}$$

$$\Delta\omega_m = \frac{(\omega_{2i} - \omega_{1o}) - (\omega_{2o} - \omega_{1i})}{\ln\frac{(\omega_{2i} - \omega_{1o})}{(\omega_{2o} - \omega_{1i})}} \tag{9}$$

where ω represents the humidity (kg/kg); subscripts 1 and 2 represent streams 1 and 2, respectively; subscripts i and o represent the inlet and outlet, respectively; and V is the stream volume flow (m^3/h). Pe ($kg\ m^{-2}\ s^{-1}$) was calculated as follows:

$$Pe = \frac{\Delta W}{A} \tag{10}$$

RESULTS AND DISCUSSION

Morphological study

For the substrate of composite membranes, the surface pore size of porous membranes is closely related to the formation of a skin layer on the substrate. The pore diameter and porosity are important parameters for characterizing the microstructure of membranes. Therefore, the prepared membranes were characterized by morphological analysis and N_2 sorption testing.

SEM analysis

The surface morphologies of different membranes by SEM are presented in Figure 2. The surfaces of the membranes with PEG were porous. When 1.2% PEG-2000 was used in the casting solution, many

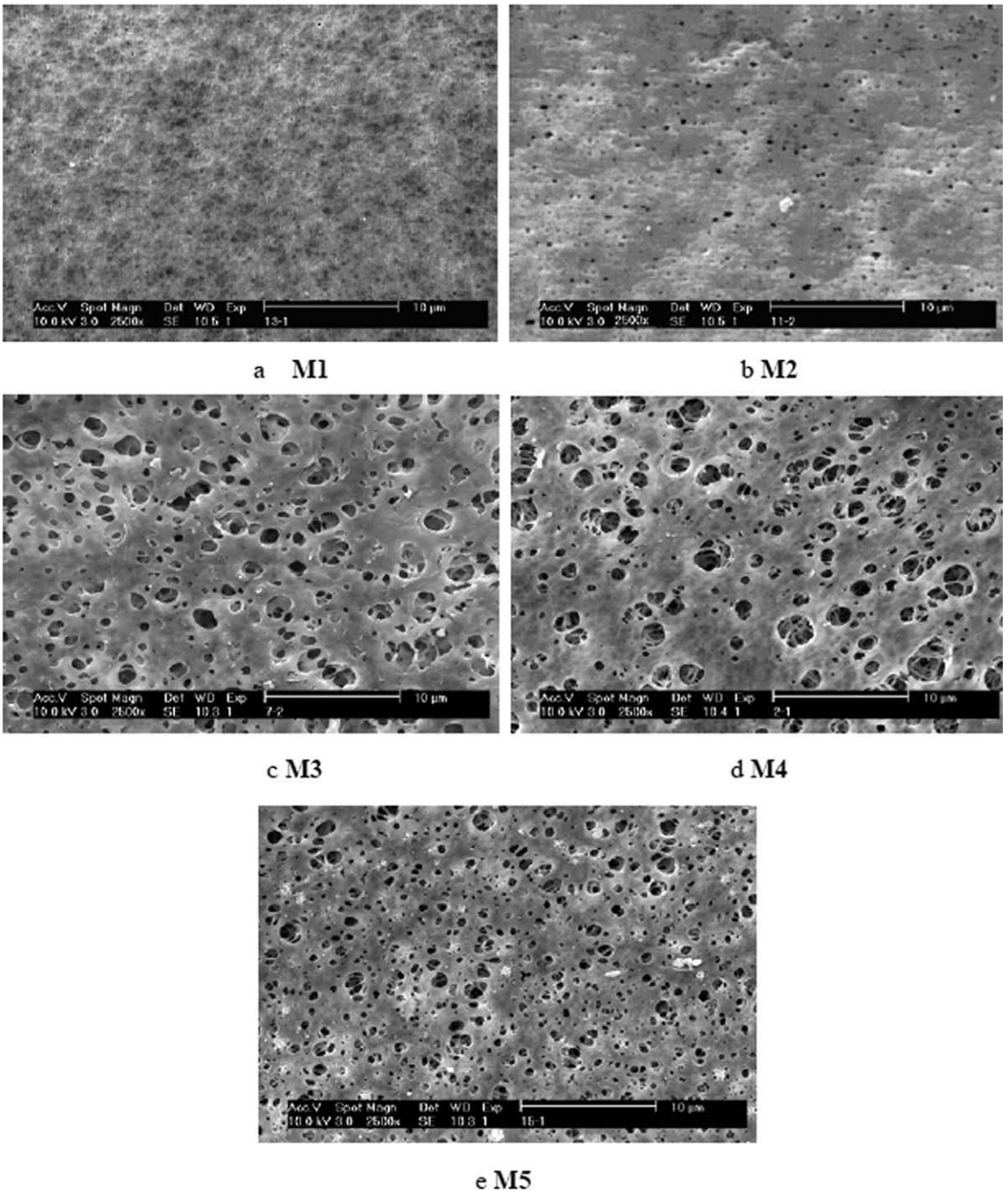

Figure 2 SEM graphs of the surface morphology of the different membranes.

pinholes were observed on the surface of the membrane [Fig. 2(a)]. As the PEG concentration increased, the surface pores enlarged, and the membrane surface became more porous. This can be explained by the thermodynamic effect of PEG. The formation of the top surface may have been due to demixing of the casting solution by means of nucleation and growth of the polymer-rich phase. As is well known, hydrophilic PEG in a casting solution acts as a nonsolvent for PVDF. The addition of PEG causes lower thermodynamic stability of the casting solution and thus accelerates phase separation. Therefore, with an increasing amount of PEG, the enhanced demixing rate at the interface leads to the rapid collapse of polymer chains and the formation of larger gaps between collapsed chains. A similar trend was also observed in a PSf/*N*-methylpyrrolidone (NMP)/PEG system.[22]

In addition, the surface pore size decreased with an increase in the PEG molecular weight. The

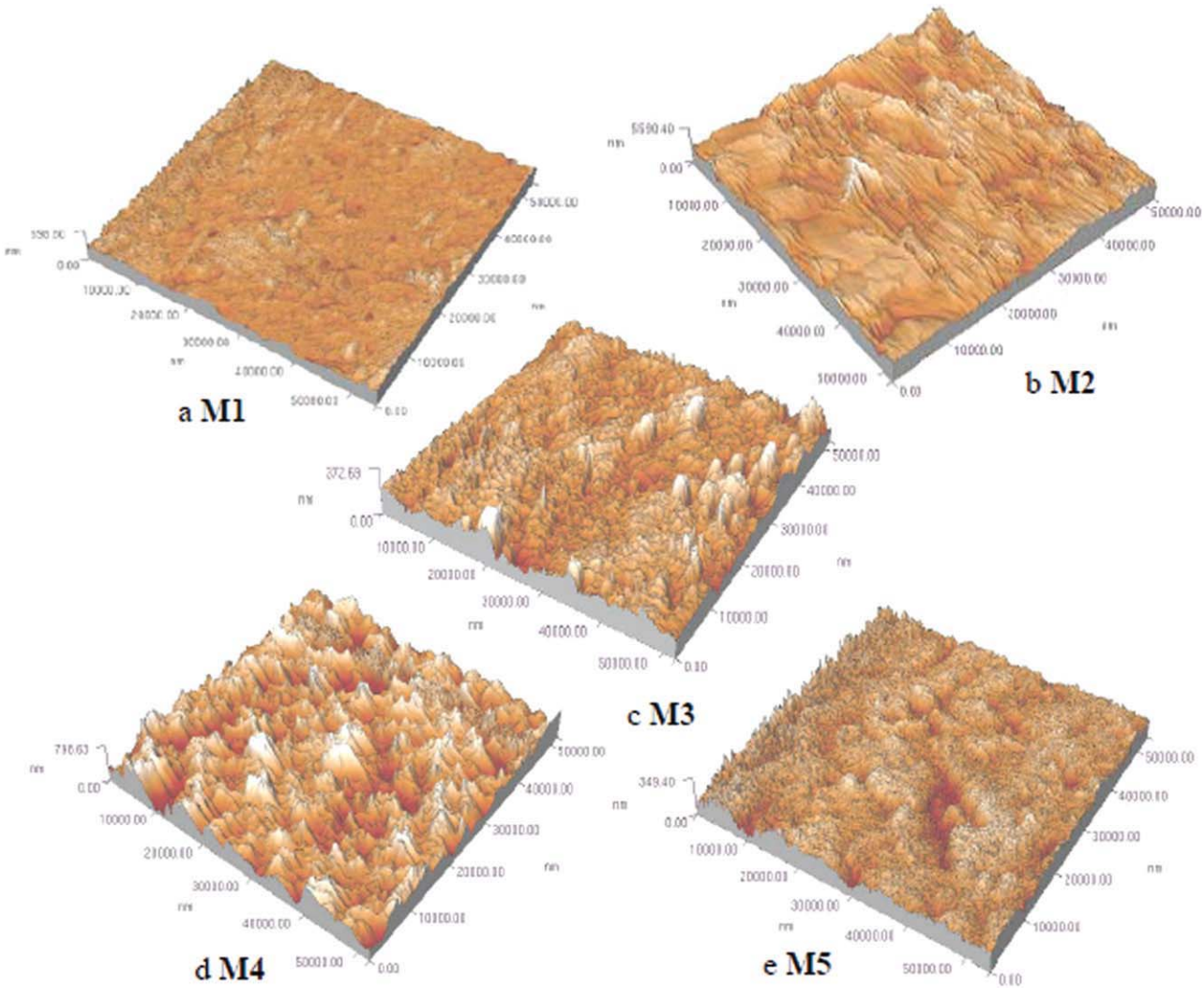

Figure 3 AFM images of the different membranes. [Color figure can be viewed in the online issue, which is available at www.interscience.wiley.com.]

variation of the surface morphology was particularly noticeable for high-molecular-weight PEG-6000. This was attributed to the difference in the relative diffusivity and solubility of PEGs of different molecular weights. When the casting solution came into contact with the coagulation bath, there was a rapid outflow of the solvent from the casting solution to the coagulation bath, and this caused aggregation of the polymer molecules on the top layer.[23] Low-molecular-weight PEG easily reached the surface and then dissolved from the raw membrane during the process of preparation and washing. This resulted in the formation of a porous surface. On the contrary, high-molecular-weight PEG needed more time to reach the surface because of the low diffusion rate and was hardly washed out because of the poor solubility; it therefore led to the formation of a dense surface with a smaller pore size. Similar results were reported by Jung et al.[24] with polyacrylonitrile membranes and by Idris and Jet[25] with cellulose acetate membrane.

AFM analysis

The surface topographies of various membranes were observed with AFM. As shown in Figure 3, the nodules were observed as bright, high peaks, whereas the pores were seen as dark depressions. The AFM image clearly shows that the membrane prepared with a 1.2% PEG concentration had a relatively smooth surface. As the PEG concentration in the casting solution increased, the surface of the membrane had more grains and became rougher. Moreover, with an increase in the molecular weight of PEG, the grain size of the membrane surface decreased, whereas the number of grains increased. Generally, the pore size depends on the size of aggregated particles or macromolecules, nodules, or

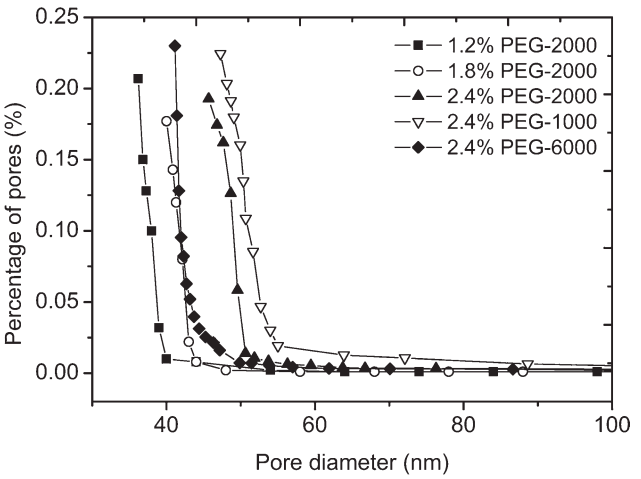

Figure 4 Pore size distributions for membranes with different PEGs.

nodule aggregates.[26] As described by Zheng and Matsuura,[27] the increase in the pore size can be roughly estimated from the increase in the roughness and size of aggregated particles on the top surface. Therefore, this variation of the surface topography indicates that an increasing concentration of PEG and a decreasing molecular weight of PEG resulted in membranes with large pore sizes, and this is quite consistent with the SEM observations.

ASAP analysis

The pore size distributions of the obtained membranes (M1–M5) were determined according to eq. (4) and are presented in Figure 4. In all cases, most pores were distributed in the range of 35–50 nm. However, the smaller pores were not determined because the vapor-transport property was greatly dependent on larger pores. This was due to the fact that the transport rate through the membranes was directly proportional to the fourth power of the pore radius (based on the Hagen–Poiseuille equation). Moreover, the pore size distribution shifted to a large pore size with the concentration of PEG increasing and to a small pore size with the molecular weight of PEG increasing.

The average pore diameters and porosity of different membranes were calculated with eqs. (5) and (6) and are listed in Table II. With an increase in the concentration of PEG, the average pore diameter increased from 35.1 to 44.6 nm, and the porosity increased from 38.0 to 54.2%. This indicated that an increasing amount of PEG resulted in more porous membranes. This variation could be attributed to the thermodynamic effect of PEG. In contrast, with the molecular weight of PEG increasing, the average pore diameter slightly decreased, whereas the porosity increased. This may be a result of competition

TABLE II
Porosity and Average Pore Diameters of Different Membranes

Sample	PEG		Porosity (%)	Average pore diameter (nm)
	Molecular weight	Concentration (%)		
M1	2000	1.2	38.0	35.1
M2	2000	1.8	47.3	40.3
M3	2000	2.4	54.2	44.6
M4	1000	2.4	52.3	46.9
M5	6000	2.4	57.8	42.5

between the thermodynamic and rheological effects of PEG. The addition of PEG caused thermodynamic enhancement of the phase separation. On the other hand, it also increased the viscosity of the solution (rheological effect), as previously observed,[22] and caused kinetic hindrance against phase separation. As the molecular weight of PEG increased, the rheological effect overweighed the thermodynamic effect. The increasing viscosity of the solution slowed the precipitation rate and thus suppressed the formation of macrovoids.[28] Meanwhile, the highly viscous solution increased the ratio of nonsolvent inflow to solvent outflow according to the theory suggested by Young and Chen[29,30] and thus yielded a more porous membrane. Therefore, the addition of higher molecular weight PEG yielded a membrane with a smaller pore size and higher porosity. A similar trend was observed for PSf/PEG/NMP and PSf/PVP/NMP systems.[16,18]

Moisture-transport performance

The moisture-transport performance of the obtained membranes was evaluated in the test rig (Fig. 1) in terms of *K* and *Pe*.

The influence of the concentration and molecular weight of PEG on *K* under different air flows is shown in Figures 5 and 6, respectively. The *K* value

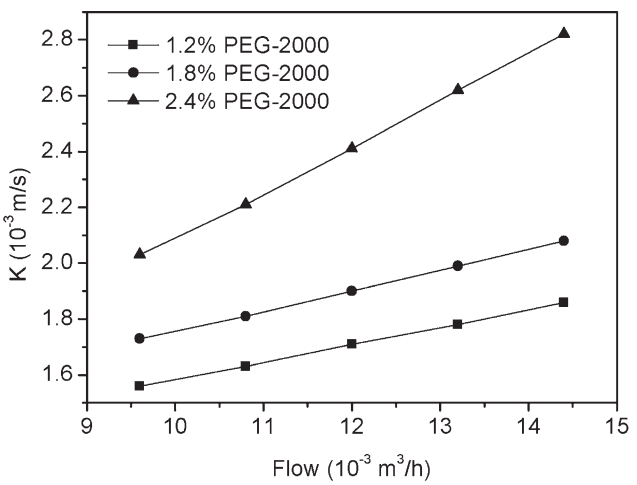

Figure 5 Effect of the PEG concentration on *K*.

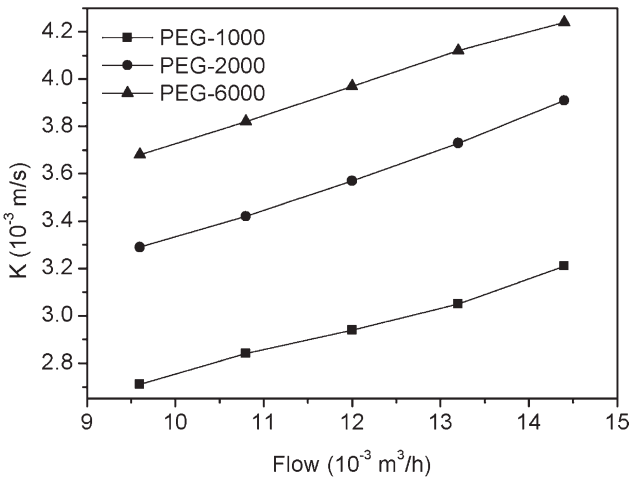

Figure 6 Effect of the PEG molecular weight on *K*.

increased with increases in the concentration and molecular weight of PEG. As previously reported,[31] *K* is defined as the inverse of the moisture-transport resistance in the exchanger. The moisture-transport resistance in the exchanger is determined by the boundary layer resistance on the humid air side, the membrane resistance, and the boundary layer resistance on the dry air side. The boundary layer resistances of the different membranes were the same because the working conditions were the same. As a result, the increasing value of *K* safely demonstrated that PEG reduced the resistance through the membranes. In general, high porosity in a membrane leads to low resistance and enhances the transport of water vapor through the membrane.[31] The improved *K* values were a result of the increasing porosity, as discussed in the ASAP analysis.

The influence of the concentration and molecular weight of PEG on *Pe* under different air flows is presented in Figures 7 and 8, respectively. *Pe* showed an increasing trend similar to that of *K* with

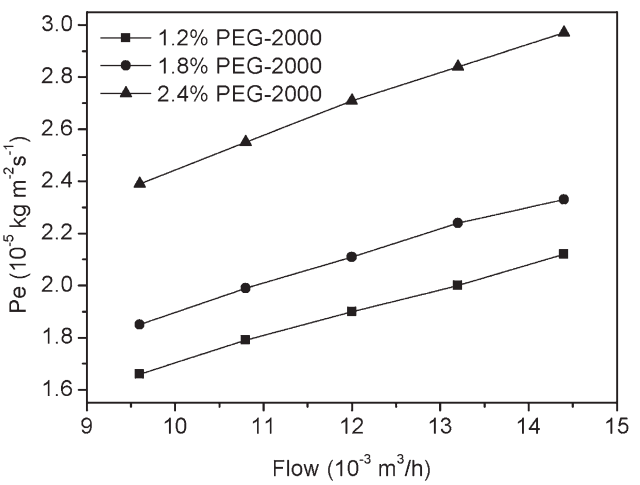

Figure 7 Effect of the PEG concentration on *Pe*.

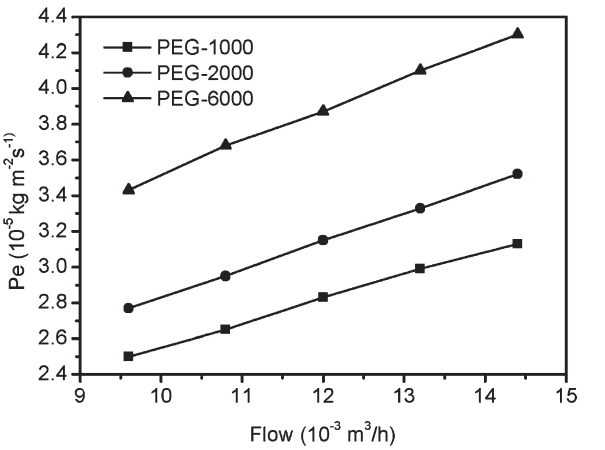

Figure 8 Effect of the PEG molecular weight on *Pe*.

increases in the concentration and molecular weight of PEG. For instance, under an air flow of 12 m^3/h, the permeation rate increased from 2.11×10^{-5} to 2.74×10^{-5} kg m^{-2} s^{-1} when the PEG concentration in the casting solution increased from 1.8 to 2.4%. Also, the permeation rate increased from 3.15×10^{-5} to 3.87×10^{-5} kg m^{-2} s^{-1} with an increase in the molecular weight of PEG from 2000 to 6000. The increasing moisture permeation was largely attributed to the increasing porosity. As described previously, the introduction of PEG increased the porosity and thus resulted in reduced membrane resistance. The low resistance was favorable for moisture transport.[31] It is reasonable that a membrane prepared with high-molecular-weight PEG at a high concentration in the casting solution would have a better *Pe* value.

CONCLUSIONS

Porous PVDF membranes with various morphologies were fabricated by phase inversion through changes in the concentration and molecular weight of PEG. A porous surface with a large pore size was formed, and the pore diameter and porosity increased with the concentration of PEG increasing. High-molecular-weight PEG led to a decrease in the surface pore size and the average pore diameter but an increase in the porosity. The moisture-transport performance of PVDF membranes was improved significantly with increases in the concentration and molecular weight of PEG. When PEG-6000 in a casting solution was used as an additive at a 2.4% concentration, the membranes showed the best moisture permeability.

References

1. Metz, S. J.; Van de Ven, W. J. C.; Potreck, J.; Mulder, M. H. V.; Wessling, M. J Membr Sci 2005, 25, 129.

2. Ito, A. J Membr Sci 2000, 175, 3542.
3. Kojima, T.; Shimizu, H.; Ito, A. J Jpn Petrol Inst 2004, 47, 403.
4. Li, J. L.; Ito, A. J Membr Sci 2008, 325, 1007.
5. Zhang, L. Z. J Membr Sci 2006, 276, 91.
6. Pan, C. Y.; Jensen, C. D.; Bielech, C.; Habgood, H. W. J Appl Polym Sci 1978, 22, 2307.
7. Hu, H.; Jia, J.; Xu, J. J Appl Polym Sci 1994, 51, 1405.
8. Zhang, L. Z.; Wang, Y. Y.; Wang, C. L.; Xiang, H. J Membr Sci 2008, 308, 198.
9. Aranda, P.; Chen, W. J.; Martin, C. R. J Membr Sci 1995, 99, 185.
10. Zhang, L. Z. Dehumidification Technology; Chemical Industrial Press: Beijing, China, 2001.
11. Liu, L.; Chen, Y.; Li, S. G.; Meng, M. C. Sep Purif Technol 2001, 36, 3701.
12. Yeo, H. T.; Lee, S. T.; Han, M. J. J Chem Eng Jpn 2000, 33, 180.
13. Mosqueda-Jimenez, D. B.; Narbaitz, R. M.; Matsuura, T.; Chowdhury, G.; Pleizier, G.; Santerr, J. P. J Membr Sci 2004, 231, 209.
14. Jung, B.; Yoon, J. K.; Kim, B.; Rhee, H. W. J Membr Sci 2004, 243, 45.
15. Yoo, S. H.; Kim, J. H.; Jho, J. Y.; Won, J.; Kang, Y. S. J Membr Sci 2004, 236, 203.
16. Chakrabarty, B.; Ghoshal, A. K.; Purkait, M. K. J Membr Sci 2008, 315, 36.
17. Uragami, T.; Naito, Y.; Sugihara, M. J Polym Bull 1981, 4, 617.
18. Idris, A.; Zain, N. M.; Noordin, M. Y. Desalination 2007, 207, 324.
19. Chakrabarty, B.; Ghoshal, A. K.; Purkait, M. K. J Membr Sci 2008, 309, 209.
20. Chakrabarty, B.; Ghoshal, A. K.; Purkait, M. K. J Colloid Interface Sci 2008, 320, 245.
21. Barrett, E. P.; Joyner, L. G.; Halenda, P. P. J Am Chem Soc 1951, 73, 373.
22. Kim, J. H.; Lee, K. H. J Membr Sci 1998, 138, 153.
23. Chuang, W. Y.; Young, T. H.; Chiu, W. Y.; Lin, C. Y. Polymer 2002, 41, 5633.
24. Jung, B.; Yoon, J. K.; Kim, B.; Rhee, H. W. J Membr Sci 2004, 243, 45.
25. Idris, A.; Jet, L. K. J Membr Sci 2006, 258, 920.
26. Singh, S.; Khulbe, K. C.; Matsuura, T.; Ramamurthy, P. J Membr Sci 1998, 142, 111.
27. Zheng, Z. X.; Matsuura, T. J Colloid Interface Sci 1991, 147, 307.
28. Wienk, I. M.; Boom, R. M.; Beerlage, M. A. M.; Bulte, A. M. W.; Smolders, C. A. J Membr Sci 1996, 113, 361.
29. Young, T. H.; Chen, L. W. J Membr Sci 1991, 57, 69.
30. Young, T. H.; Chen, L. W. J Membr Sci 1991, 59, 169.
31. Zhang, L. Z. Sep Purif Technol 2006, 41, 1565.